Journal of Harbin Engineering University
ISSN: 1006-7043
Vol 44 No. 12
December 2023

Effect of Time Step in Return Bend Upstream & Downstream Flow for Bubbly Flow Pattern and Pressure Drop Characteristics: A CFD Analysis

Ashutosh kumar[1*] and Mukesh Sharma[1]
[1] Birla Institute of Technology Mesra, Ranchi, India.

Abstract
A return bend pipe is designed to avoid the need for an abrupt change in direction and orientation during the concurrent oil-water flow. For different sets of the superficial velocities of kerosene with water, the Volume of Fluid (VOF) model based on the Eulerian-Eulerian approach provided in Fluent was used to determine the flow pattern and local pressure drop characteristics. The present work deals with kerosene-water flow in a return tube bend (curvature $2R/d$ of 8) that connects two 0.15-m long horizontal tubes. The two-phase flow can be adjusted to either an upward or downward direction, and the bend is in a horizontal position. The trend between numerically calculated pressure drops and experiments appears to be satisfactorily matching. The outcomes provide appropriate operational parameters for creating the U-bend pipe fitting.

Conclusion
Kerosene and water through the return bend has been simulated to visualize the Bubbly flow in the present study. The CFD software FLUENT 2020 R1 has been used to create 3D models. The confirmation of the models with experiments reported by Sharma et al. (2011) indicates a good agreement for return bend. The significant conclusion is highlighted in the following:

- The effect of buoyancy is more at lower water and kerosene superficial velocity as compared to inertial and viscous force.
- On higher superficial velocity more bubbles observed in upstream flow at the same time step.
- The direction of flow has much influence on Phase inversion, water to oil inversion takes place early downstream of flow at higher superficial velocity.
- A higher pressure drop was obtained at the minimum superficial velocity of oil in the return bend section.

Keywords: Liquid-liquid Flow, Return bend, Flow pattern, Time step. Pressure drop.

Introduction

Pipe bends are armature elements that are used to divide the flow mixture by altering the flow direction. These essential pipe fittings are used in a variety of technical applications, including the transportation of petroleum, the petrochemical industry, ventilation, air conditioning, water supply drainage, refrigeration, and nuclear reactors. The shape of the bend has an impact on downstream flow regimes. A return bend pipe unites straight parallel pipes and saves installation space in process industries concerning the continuous transit of water and oil through pipelines(Pietrzak et al.,2014).

Most recent work for the bend pipe test section reported by Magnini et al.(2018) and Tan et al.(2018) in which inclination as reported by Habachi et al.(2009), Sharma et al.(2011) Pieztrak et al.(2014) Biswas et al.(2015), Jiang et al.(2018) and Magnini et al.(2018) summaries are depicted in table 1. Sharma et al. (2011) reported that the pressure drop in the bend was greater than that in the U bend as compared to Π bend. This bend has two right-angled elbows that may affect the hydrodynamics and fouling properties differently.

In the bends due to centrifugal force division of the two phases brings the complexity of two-phase flow. Simmons (2001) reported that the drop generation mechanism occurs when the Froude number is high or the submerged depth is low (Chinaud et al., 2016). Piela et al. (2009) reported that drop is the smallest part of the dispersed phase usually smaller than 1mm. Regarding the size of the drop important literature provided by Simmons et al.(2001) Kitagawa et al.(2007), Piela

et al. (2006 & 2009), Morgan et al.(2012 & 2013), and Rodriguez et al.(2012). They experimented with a two-phase flow of water with silicon oil, Shell macron ExcolD80, Kerosene, and Aqueous potassium respectively. Maximum drop diameter obtained at low concentration of dispersed phase (Simmons et al., 2001). According to Kitagawa et al. (2007) diameter deviation and location of the droplet strongly depends on the balance of buoyancy force, Drag force, and pressure gradient acting on the droplet in the radial direction. The break-up of the jet emerging from the injector holes, which relies on the jet exit velocity, determines the drop size distribution (Piela et al., 2006). For a fixed superficial velocity (U_m) the droplet diameter increases at a constant rate with increasing oil input fraction up to ϕ_{in} =0.5. After increasing from 0.5 the average droplet diameter decreases, At low oil fractions, the change in superficial mixing velocity does not affect the interface level; however, at high oil fractions, the interface height from the channel bottom decreases as the superficial mixing velocity rises (Morgan et al.,2012 and Rodriguez et al.,2019). If the oil cut is increased keeping the water superficial velocity constant mixture velocity also increased (Rodriguez et al., 2019). For horizontal flow stratification of the droplet was observed at low mixture velocity. A higher mixture is required for fully developed flow in large-diameter pipes **(**Piela et al., 2009). It demonstrates that as the bubbles in the bubbly flow migrate to the inside of the bend, and conversely, under some circumstances, the heavier phase moves to the inside of divided flows (a phenomenon known as film inversion). The pump and length of the pipe do not influence the morphology of the dispersion when the growth of multiple drops is present and this is a slow process. (Piela 2006). A probability distribution is not affected by droplet volume fraction but depends on the pattern generation of the droplet (Kitagwa et al., 2007)**.** The occurrence of particles or droplets increases the μ_o of a suspension, and the μ_o for dilute suspensions is dependent on the particle percentage (Tan et al., 2019). The viscosity of a solution rises when particles or droplets are present, and it depends on the particle fraction for diluted suspensions.

Phase inversion is the process whereby an oil in water transitions from its continuous phase to its dispersed phase and back again as a result of a change in operational conditions (Viggiano et al.,2018 and Piela et al.,2006) that helps to determine the amount of force that must be used to move the liquid from one location to another, as well as the influence of flow variables including temperature, mixture velocity, interfacial tension, mean drop size and drop distribution, etc (Welch et al., 2002). Due to the coalescence of the dispersed phase and the break-up of the continuous phase, mixing velocity inversion happens when we increase the water percentage (Piela et al., 2006). Turbulence pressure fluctuations, which are related to the geometrical features of the contact, cause the drop to break apart and coalesce (Viggiano et al., 2018). The probability of their coalescence increases as the extent of the drop increases, and inversion occurs (Piela et al., 2006).

Computational fluid dynamics (CFD), which can provide a wealth of information on flow characteristics that are challenging to measure experimentally in some complex devices, has attracted a great deal of interest as a result of recent developments in machines and computer calculators. (Chekifi et al.,2021).Jiang et al. (2014) mentioned that currently, three numerical models the volume of fluid (VOF) model, the Eulerian model, and the Mixture model, are utilized to tackle two-phase flow issues. The VOF approach, for monitoring fluid-fluid interfaces that do not interpenetrate, is taken into consideration in the current study since it is both reasonably simple and accurate. They simulated a horizontal flow with a density difference utilizing the VOF model to take a look at the effect of buoyancy (Magnini et al., 2018). Chekifi. (2018) simulated the droplets breakup in trapped channel devices using the VOF Method. According to Santos et al. (2019), two-phase flows of an incompressible fluid with interface tension may be simulated using the volume of fluid technique, the level set method, the phase field approach, and the front tracing method. They employed the level set model in the horizontal pipe together with the k- epsilon model and RANS in considering the flow regime for the petroleum sector.

The prior literature makes it clear that most studies on return bends were done experimentally. Limited computational studies on return bends are available; however, almost nothing is known about the effect of superficial velocity in the return bends for upstream and downstream of the pipe at a different time step. Therefore, it is worth exploring the flow phenomenon to understand the inversion from water to kerosene and vice versa through the return bends, and also to investigate the pressure drop at return bend at different superficial velocities because in industrial applications oil-water flow is usually transported through return bends.

Sr.No.	Author (Year)	Diameter (mm)	Length (mm)	Oil Physical Properties (Kg/m^3, mPas)	Pipe material	Superficial Velocity (or mixture velocity) (m/s)	Flow direction	Study Aims	Pressure gradient
1	Piela et al. (2006)	16	6	δ_{water} =998 δ_{oil}=N/A	Acrylic	U_m = 2 & 3.5	Upward & Downward	Through a horizontal conduit, phase inversion in oil and water was studied.	YES
2	Tan et al. (2010)	50	2.1	δ_{water}=998 $\delta_{kerosene}$=787	Perspex	U_{sk}=0 to 0.036	N/A	Studied to modify the mass flow rate	N/A
3	Sharma et al. (2011)	12	4	δ_{water} = = 998 δ_{oil}=860	Acrylic	U_{sk}=0.075-	Upward & Downward	Understood the hydrodynamics of low viscous oil.	N/A
4	Chao Tan et al. (2010)	50	17	δ_{water} = = 998 δ_{oil}=856	Stainless	N/A	Upward	Horizontal oil-water phase measurement	YES
5	Zhang et al. (2013)	25	1.2	δ_{water}= 998 δ_{oil}=830	Perspex	U_{so}=	Upward & Downward	Studied the experimental validation of phase hold-up.	N/A
6	Fan Jiang et al. (2014)	12	4	δ_{water} =998 δ_{LAN}15machine =	N/A	V_{so}=0.15	Upward & Downward	Investigated the VOF, Standard k-e, and CSS Models.	N/A
7	Pietrzak et al. (2014)	16,22,30	1.5,3.5,	δ_{water} = 998 δ_{oil}= 841	Plexiglass	U_{so}=0.014	Upward	Understood the hydrodynamics of CAF through pipe bends.	N/A
8	Biswas et al. (2015)	2	1	δ_{water} =998 $\delta_{kerosen}$ =787	Glass	U_m =0.26 to	Upward	Studied to use of bends for enhanced	YES

								mass transfer.	
9	Voulgaropoulus et al. (2017)	26	4	δ_{water} =1000 $\delta_{industrial=}$	Acrylic	U_m=0.36	N/A	Qualities of liquid-liquid flow that pertain to acquired flow and liquid separation.	N/A
10	Jiang et al. (2018)	12	N/A	δ_{water} =998δ_{oil} =960	CS, GS, SS,	U_{so} =0.6	Up-flow	Investigated the influence of oil	N/A

Table-1 Summary of previous work

2 Mathematical formulation

2.1 A physical and computational model

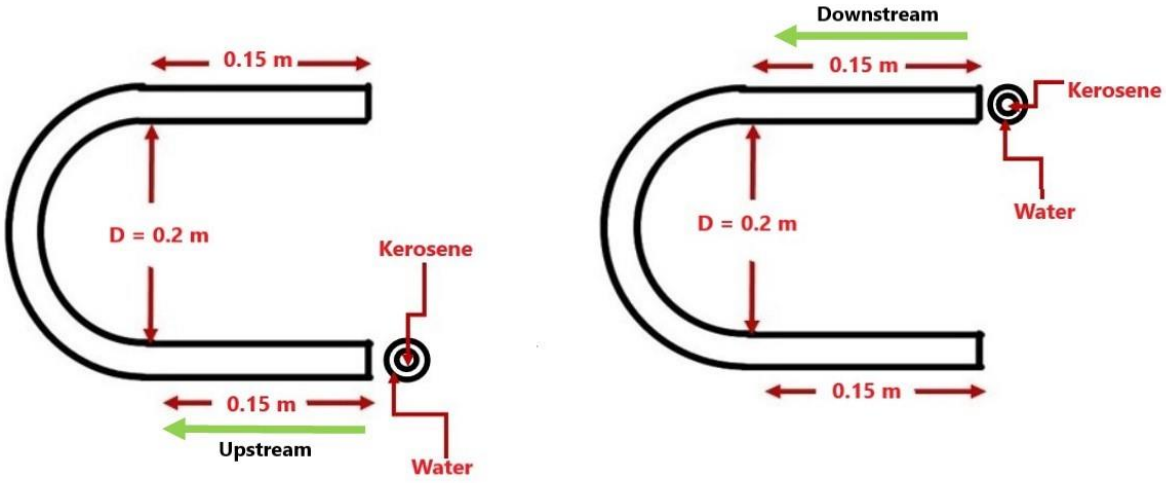

generate the tube (D_1 = 0.0254 m & D_2 = 0.0127 m. Curvature is $2R/d$ of 8 that connects two 0.15-m long horizontal tubes. Kerosene was chosen for the second phase while water was chosen as the primary phase. Information is provided in Table 1. The viscosity-affected near-wall region was taken into consideration using the k-epsilon realizable model with enhanced wall treatment. (Roul et al., 2010), which increases the model's accuracy by simulating turbulence. Gravity was also considered because the phases' varying densities indicate flows at each target site since the inlet was designed as a velocity inlet. The outlet border was roughly estimated using a pressure outlet (López et al., 2016).

Table 2 Physical properties of the test fluid (Sharma et al., 2011).

Test Fluid	Density (kg/m^3)	Viscosity (kg/m-s)	Surface tension(N/m)
Kerosene	780	0.0012	0.027
Water	998.2	0.001003	0.072

2.1Assumptions

In contrast to the converging entry that occurs in real-world situations, this simulation is predicated on the assumptions of constant liquid characteristics, and coaxial liquid entry of an immiscible liquid pair.

2.2 Governing equations

Equations that are governed by the being there of numerous phases, space-departure interfaces, time, different scales, modeling of multiphase flow, and a significant number of interacting phenomena require special treatment (Multiphysics) in the fluid. Different strategies are used for different types of flow patterns. The Eulerian-Eulerian method may simulate a separated flow with a clearly defined interface (Kaushik et al., 2012). For two-phase modeling, the Volume of Fluid (VOF) technique based on the Eulerian-Eulerian technique provided by FLUENT is a good substitute for the hydrodynamic behavior of flow patterns (Ghosh et al., 2011). In this method, a single set of momentum equations is shared by both fluids the models include the continuity equations and Navier- stokes and can be written as follows:

$$\alpha_0 + \alpha_\omega = 1 \quad (1)$$

$$\frac{\partial \rho}{dt} + \nabla \cdot (\rho \vec{v}) = 0 \quad (2)$$

$$\frac{\partial (\rho \vec{v})}{dt} + \nabla(\rho \vec{v}\vec{v}) = -\nabla p + \nabla.[\mu(\nabla \vec{v} + \nabla \vec{v}^T)] + \rho \vec{g} + \vec{F} \quad (3)$$

$$\frac{\partial (\rho k)}{dt} + \nabla(\rho k \vec{v}) = \nabla\left(\frac{\mu_t}{\sigma}\nabla k\right) + 2\mu_t E_{ij} E_{ij-\rho\varepsilon} \quad (4)$$

$$\frac{\partial (\rho k)}{dt} + \nabla(\rho k \vec{v}) = \nabla\left(\frac{\mu_t}{\sigma}\nabla k\right) + C_{1\varepsilon}\frac{\varepsilon}{k} 2\mu_t E_{ij} E_{ij-C_{2\epsilon}} \rho \frac{\varepsilon^2}{k} \quad (5)$$

$$\mu_t = C_\mu \rho \frac{k^2}{\varepsilon} \quad (6)$$

E_{ij} is defined as

$$E_{ij} = \frac{1}{2}\left(\frac{\partial v_i}{\partial x_j} + \frac{\partial v_j}{\partial x_i}\right) \quad (7)$$

The constants are $\sigma_k = 1$, $\sigma_\varepsilon = 1.3$, $C_{1\varepsilon} = 1.44$, and $C_{2\varepsilon} = 1.92$, $C_\mu = 0.09$,

2.4 Boundary conditions:

2.4.1ForInlet

All the set of fluid inlet superficial velocity is specified from the same surfaces, from the core side kerosene and lubricating oil separately flowing of the horizontal pipe and water from the annular side of the inlet pipe(Dasari et al., 2013) as seen in Figure 1. The initial condition is as follows:

$V_x = V_{sk,} \& V_{sw}$

At $0 \le r \le 0.012$m $V_x = V_{sw}$ hydraulic diameter and intensity are 0.012m, and 5 percent respectively.

$0.012 \le r \le 0.025$ m $V_x = V_{sk} \& V_{sw}$

Hydraulic diameter and Intensity are 0.012 m and 5 percent respectively, at $0 \le r \le 0.012$ m,

At 5% turbulent intensity and of 0.012 m. hydraulic diameters a pressure outlet is set at the pipe's downstream outlet.

2.4.2 For Wall

On the pipe's wall, with no penetration ($V_r=0$) and no slip ($V_x=0$) condition is utilized.

2.4.3 For Outlet

2.5 Methodology

Numerous techniques are used to discretize the governing equations. Using the Second-order upwind momentum equations are discretized

while the continuity equation is discretized using the PRESTO! Method. (Lopez et al., 2016), Using the Coupled algorithm, the pressure-velocity coupling is solved. Overall, these methods gave the model stability, remove false diffusion, and provide convergence. It uses a transient simulation when the residual for each variable is reduced by a factor 0.001 times its initial residual value. A transient state with a time step size of 0.0001 s was created to compute the fully developed solution to compare the outcomes and mixing behavior of the flow.VOF was employed to replicate the two phases of flow through the pipe. The hydrodynamics of the oil-water flow can be taken into account to solve a well-defined interface. The separated flow at the Eulerian-Eulerian interface can be simulated using this model. The numerical formulation provided by VOF for tracking non-interpenetrating interfaces (Jiang et al., 2014) or an extra transport equation that is highly straightforward and precise was employed in this investigation. For the phase interaction, a constant surface tension coefficient of 0.045 was utilized. The flow chart & Algorithms are shown in Figure 2.

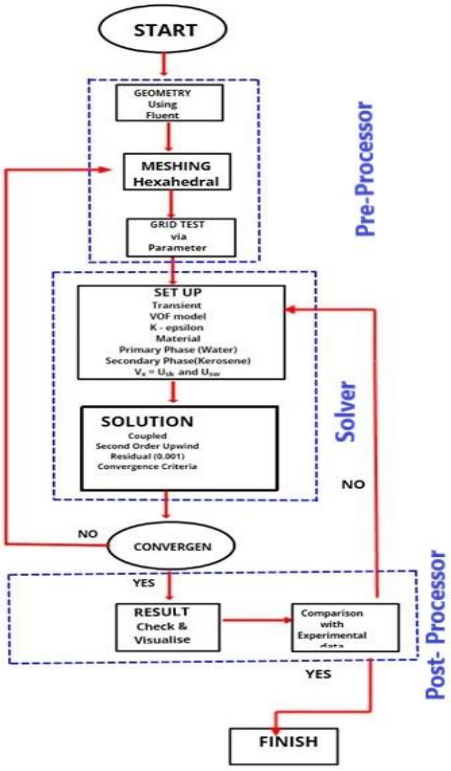

Figure 2 Algorithms and Flow chart

2.5.1The meshing of the geometry

The software ANSYS Workbench meshes the computational domain, which is shown in Figure 3. There are 32860 nodes and 29568 meshing elements in the grid. An appropriate check is carried out to maintain the grid's independence from the outcomes, details mentioned in Figure 4. For the current collection of nodes, the results demonstrate their independence and validate the current result with the Sharma et al. (2011) shown in Figure 5

Figure 3 Orthogonal Meshes for Geometry

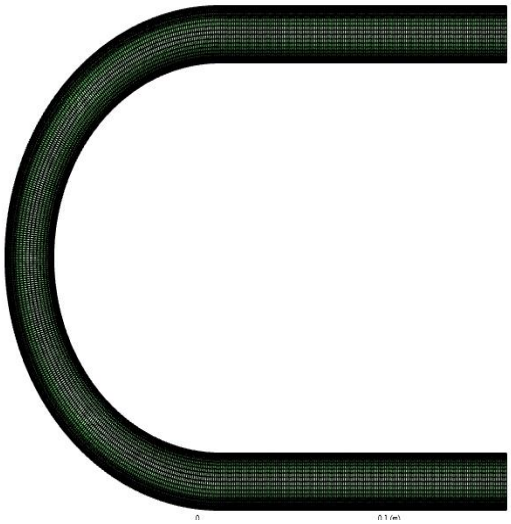

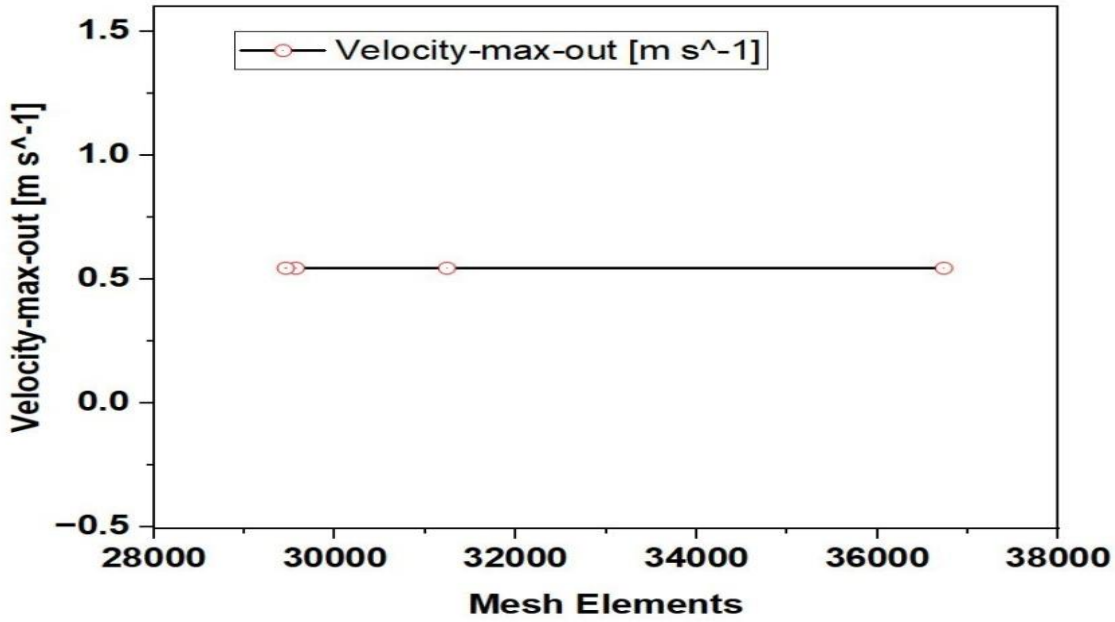

Figure 4 Grid independence test result on U_{sk}= 0.15 m/s &U_{sw} = 0.15 m/s

To confirm the simulation, the outcomes are contrasted with the experimental data reported by Sharma et al. (2011). For this, a horizontal flow U bend of pipe, and pressure gradient of hydrodynamic pressure have been superimposed and are shown in Figure 5, Similar results have been observed, with a maximum error of 7.09% in the return bend pipe.

Figure 5 Simulation results with experimental work of Sharma et al. (2011) for Horizontal Flow in return bend.

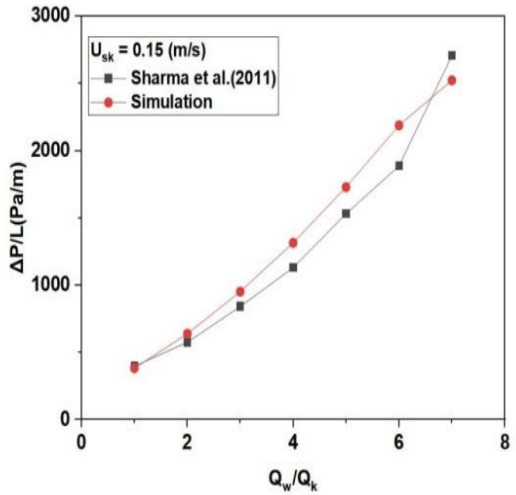

2.5.2 Wall Adhesion and Surface Tension

The VOF model incorporates surface tension force at each pair of phase contacts. In the present instance, the continuous surface force (CSF) model developed by Brackbill et al. (1992) was used. The Young-Laplace method is used to determine the surface curvature using two radii, R_1 and R_2, in orthogonal directions, and a constant surface tension coefficient, of 0.045 and 0.052 for kerosene and lubricating oil with water separately, which is an important term in the momentum equation.

$$P_2 - P_1 = \sigma\left(\frac{1}{R_1} + \frac{1}{R_2}\right) \quad (8)$$

Where on either side of the interface P_1& P_2 represent the pressure in the two fluids

3 Result and discussion

During upstream and downstream of the return bend effect of superficial velocity on the flow pattern is observed at the same time step**.** Due to the interaction of centrifugal forces on the mixture and the undeveloped flow profile in bends, the behavior of the fluid flow in bends is complex**.** When there was low oil superficial velocity and a moderate water flow rate, bubbly flow occurred. At the top of the pipe, elongated bubbles or plugs were in motion, and water was in the continuous phase. The length of the bubble or clog was equal to or greater than the pipe diameter. In the hydrodynamically produced straight flow before the curve, the bubbles/plugs were more tightly packed; at the bend and after the bend, they were less. This resulted from the bend on bubbles exerting shear pressures on them.

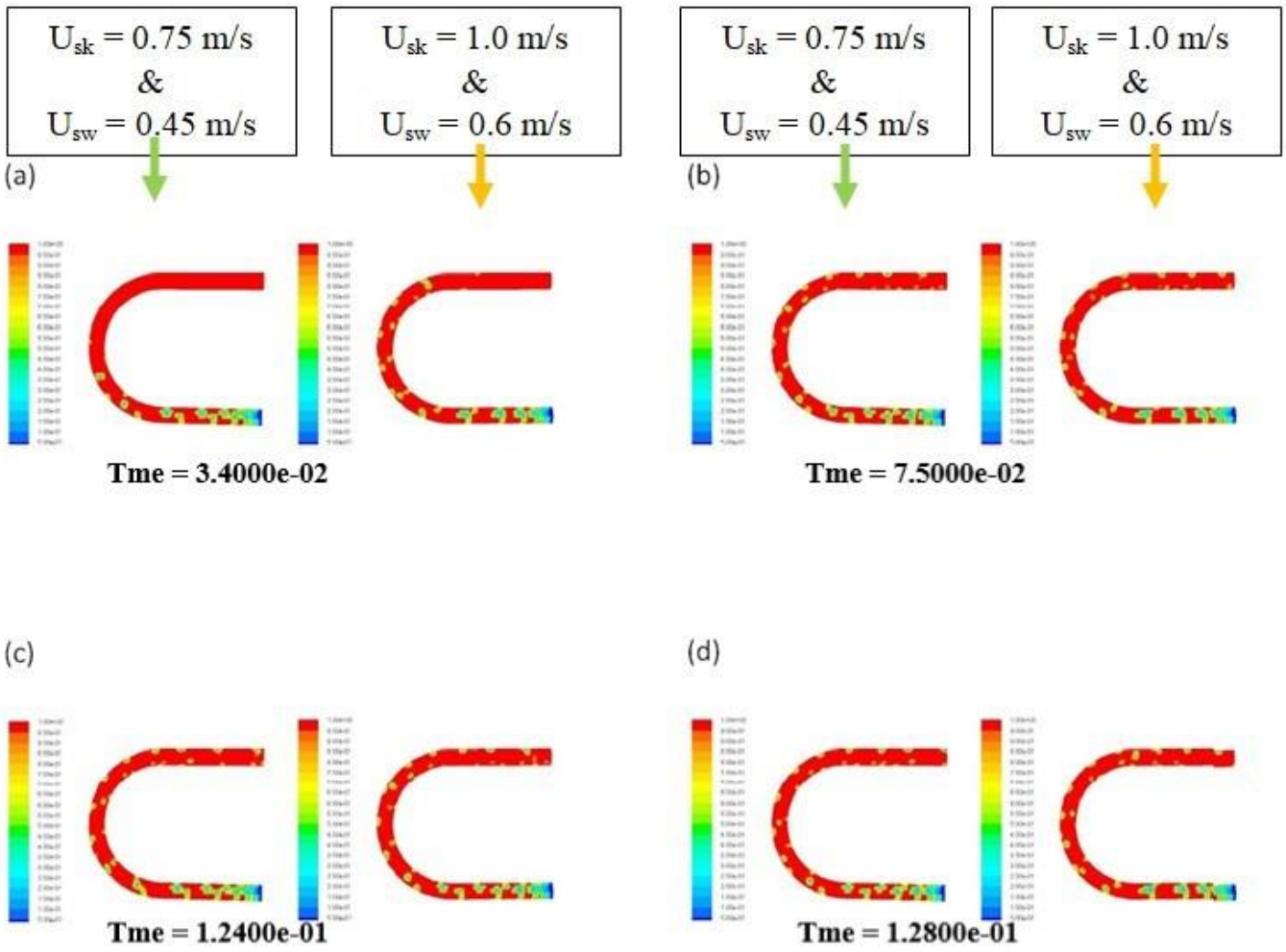

Figure 6 (a-d) Visualization for Upstream flow between U_{sk}= 0.75 m/s & U_{sw} = 0.45 and U_{sk}= 1.0 m/s & U_{sw} = 0.6 m/s at

Figure 6 (a)-(d) shows the formation of the bubble at different superficial velocity at different time step in the upstream flow, As the time step increases the formation of a bubble is more and overlap the whole tube, but at minimum time step and lower superficial velocity formation is very less as compared to higher superficial velocity shown in figure (a)

Figure 7 (a-d) Visualization made for downstream flow between U_{sk}= 0.75 m/s & U_{sw} = 0.45 and U_{sk}= 1.0 m/s

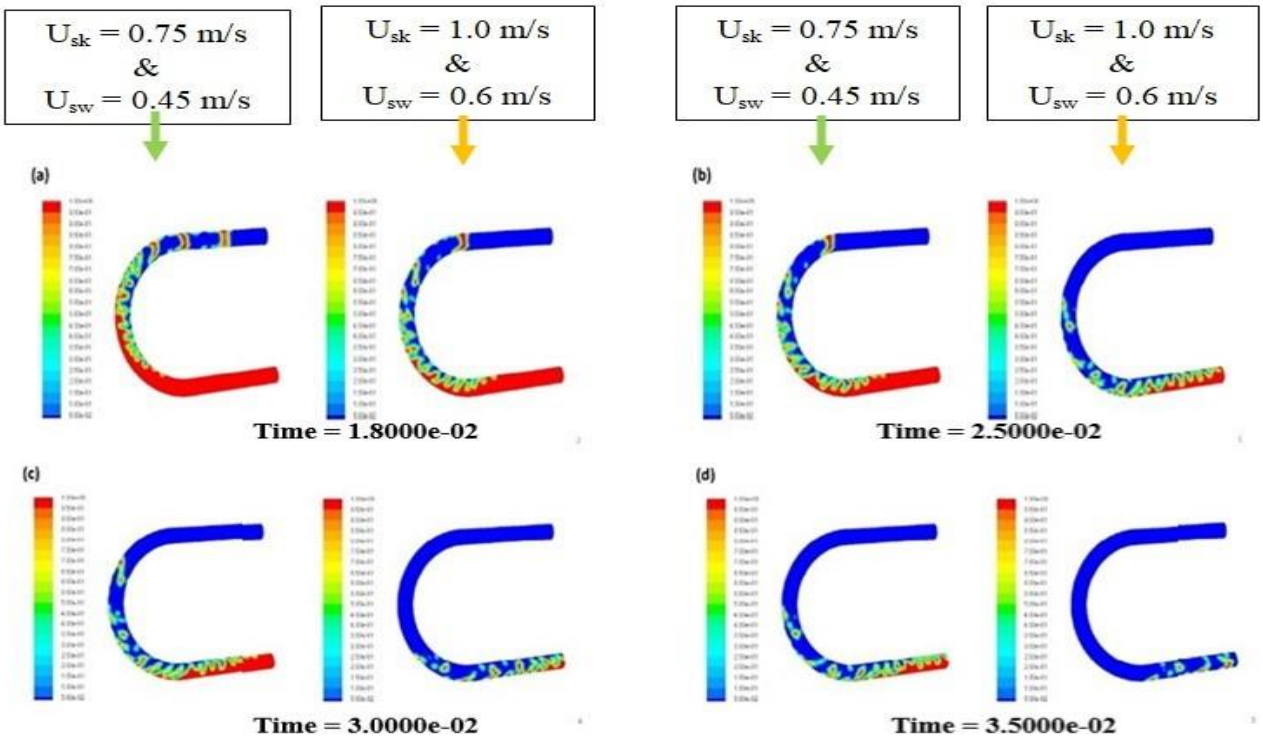

& U_{sw} = 0.6 m/s at

Similarly, Figure 7 (a)-(d) shows the formation of the bubble at different superficial velocity at different time step in the downstream flow, As the time step increases bubble formation is vanish and become a continuous flow, at higher superficial velocity formation is quicker. compare to lighter superficial velocity shown in Figure (d)

3.2 Pressure drops

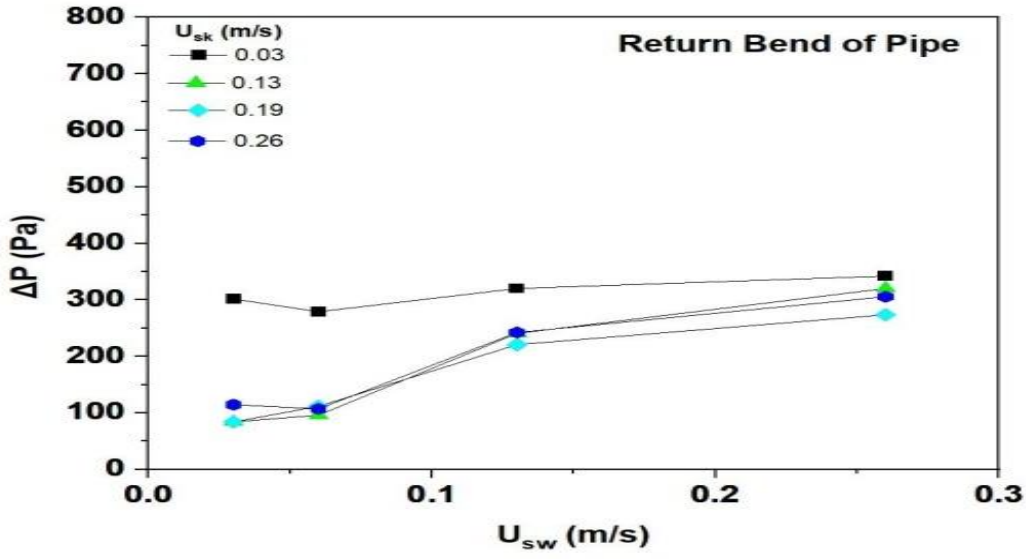

Figure 8 Maximum pressure drop is obtained at minimum superficial velocity of oil at return bend.

Figure 8 (a) illustrates the four instances of pressure drop at corresponding U_{sw} = 0.03, 0.06, 0.13, and 0.26 m/s In return bend, the higher pressure drop is obtained at a lower superficial velocity (Ayegba et al.,2021), and for a 180^o return bend, Mondal et al. (2001) demonstrated that it is not necessarily linear.

Abbreviation

D_1	Larger diameter(m)
D_2	Smaller diameter(m)
r	Radius (m)
U_{sk}	Kerosene superficial velocity, (m/s)
Usw	Water superficial velocity(m/s)
Vx	Axial velocity (m/s)
Vr	Radial velocity(m/s)
VOF	Volume of Fluid -

Symbol

μo	Oil Viscosity (Kg/m-s)
μw	Water Viscosity(Kg/m-s)
ρ	Density(Kg/m3)
σ	Surface Tension(N/m)
ρ_w	Water Density (Kg/m^3)
ρ_o	Oil Density Kg/m^3
α_o	Oil phase -
α_w	Water phase -
$\vec{v}$	Velocity(m/s)
t	Time(S)
k	Turbulence kinetic Energy ($m^2 \cdot s^{-2}$)
μv	Dissipation rate(Kg/s4-m)
p	Pressure(N/m2)
g	Gravity acceleration (m/s2)
F	Force (N)

Acknowledgement

We gratefully acknowledge the Mechanical Engineering department at Birla institute of Technology Mesra for generously providing access to their lab fascilities, enabling the successful completion of our research

Reference

[1] Brackbill, J. U., D. B. Kothe, and C. Zemach. "A continuum method for modeling surface tension J. of Comp." (1992): 6.

[2] Biswas, Koushik Guha, Sayani Majumdar, Gargi Das, and Subhabrata Ray. "The influence of bends on liquid–liquid flow through reduced dimensions." *Chemical Engineering Journal* 281 (2015): 995-1007.

[3] Chekifi, Tawfiq. "Computational study of droplet breakup in a trapped channel configuration using a volume of fluid method." *Flow Measurement and Instrumentation* 59 (2018): 118-125.

[4] Ghosh, Sumana, Gargi Das, and Prasanta Kumar Das. "Simulation of core annular in return bends—A comprehensive CFD study." *Chemical engineering research and Design* 89, no. 11 (2011): 2244-2253.

[5] [5]Dasari, Anjali, Anand B. Desamala, Ashok Kumar Dasmahapatra, and Tapas K. Mandal. 2013. "Experimental Studies and Probabilistic Neural Network Prediction on Flow Pattern of Viscous Oil-Water Flow through a Circular Horizontal Pipe." *Industrial and Engineering Chemistry Research* 52 (23): 7975–85. https://doi.org/10.1021/ie301430m.

[6] Fan, Yijun Wang, Jiajie Ou, and Zhongmin Xiao. "Numerical simulation on oil–water annular flow through the Π bends." Industrial & Engineering Chemistry Research 53, no. 19 (2014): 8235-8244.

[7] Jiang, Fan, Yijun Wang, Jiajie Ou, and Zhongmin Xiao. "Numerical simulations on oil–water annular flow through the Π bend." *Industrial & Engineering Chemistry Research* 53, no. 19 (2014): 8235-8244.

[8] Jiang, Fan, Ke Wang, Martin Skote, Teck Neng Wong, and Fei Duan. "The effects of oil property and inclination angle on oil–water core annular flow through U- Bends." *Heat Transfer Engineering* 39, no. 6 (2018): 536-548.

[9] Kaushik, V. V. R., Sumana Ghosh, Gargi Das, and Prasanta Kumar Das. "CFD simulation of core annular flow through sudden contraction and expansion." *Journal of Petroleum Science and Engineering* 86 (2012): 153-164.

[10] Kitagawa, Atsuhide, Yoshimichi Hagiwara, and Takuro Kouda. "PTV investigation of phase interaction in dispersed liquid–liquid two-phase turbulent swirling

flow." *Experiments in fluids* 42, no. 6 (2007): 871-880.

[11] Li, Ya, Li-Qin Li, Kathrin Feldberg, Peng-Cheng Wu, Harald Schneider, Alexander R. Schmidt, and Yong-Dong Wang. "Re-appraisal of two fossil Frullaniaceae species (Marchantiophyta, Porellales) from the mid-Cretaceous Burmese amber." *Cretaceous Research* 124 (2021): 104803.

[12] López, Jorge, Hugo Pineda, David Bello, and Nicolás Ratkovich. 2016. "Study of Liquid-Gas Two-Phase Flow in Horizontal Pipes Using High-Speed Filming and Computational Fluid Dynamics." *Experimental Thermal and Fluid Science* 76: 126–34. https://doi.org/10.1016/j.expthermflusci.2016.02.013.

[13] Macias Hernandez, Manuel J., Omar Dávila-Maldonado, Ariel Guzmán-Vargas, Rogelio Sotelo-Boyás, and Liliana Zarazua-Villalobos. "CFD simulation of interfacial instability from the nozzle in the formation of viscous core-annular flow." *The Canadian Journal of Chemical Engineering* 94, no. 10 (2016): 2004-2012

[14] Magnini, M., A. Ullmann, N. Brauner, and J. R. Thome. "Numerical study of water displacement from the elbow of an inclined oil pipeline." *Journal of Petroleum Science and Engineering* 166 (2018): 1000-1017.

[15] Morgan, Rhys G., Christos N. Markides, Colin P. Hale, and Geoffrey F. Hewitt. "Horizontal liquid–liquid flow characteristics at low superficial velocities using laser-induced fluorescence." *International journal of multiphase flow* 43 (2012): 101-117.

[16] Morgan, Rhys G., Christos N. Markides, Ivan Zadrazil, and Geoffrey F. Hewitt. "Characteristics of horizontal liquid–liquid flows in a circular pipe using simultaneous high-speed laser-induced fluorescence and particle velocimetry." *International journal of multiphase flow* 49 (2013): 99-118.

[17] Osundare, Olusegun Samson, Gioia Falcone, Liyun Lao, and Alexander Elliott. "Liquid-liquid flow pattern prediction using relevant dimensionless parameter groups." *Energies* 13, no. 17 (2020): 4355.

[18] Pietrzak, Marcin, and Stanisław Witczak. "Flow patterns and void fractions of phases during gas– liquid two-phase and gas–liquid–liquid three-phase flow in U-bends." *International journal of heat and fluid flow* 44 (2013): 700-710.

[19] Pietrzak, Marcin. "Flow patterns and volume fractions of phases during liquid–liquid two- phase flow in pipe bends." *Experimental thermal and fluid science* 54 (2014): 247- 258.

[20] Piela, K., R. Delfos, G. Ooms, J. Westerweel, R. V. A. Oliemans, and R. F. Mudde. "Experimental investigation of phase inversion in an oil–water flow through a horizontal pipe loop." *International journal of multiphase flow* 32, no. 9 (2006): 1087- 1099.

[21] Piela, K., R. Delfos, G. Ooms, J. Westerweel, and R. V. A. Oliemans. "Dispersed oil–water– gas flow through a horizontal pipe." *AIChE journal* 55, no. 5 (2009): 1090-1102.

[22] Rodriguez, Oscar MH, Iara H. Rodriguez, and Jonas L. Ansoni. "An experimental and numerical study on the wall lubrication force in dispersed liquid-liquid flow." *International Journal of Multiphase Flow* 120 (2019): 103094.

[23] Tan, Chao, Xiao Li, Hao Liu, and Feng Dong. "An ultrasonic transmission/reflection tomography system for industrial multiphase flow imaging." *IEEE Transactions on Industrial Electronics* 66, no. 12 (2019): 9539-9548.

[24] Qin, Min, Kexi Liao, Sijia Chen, Guoxi He, and Shijian Zhang. "Numerical simulation of gas-liquid flow in inclined shale gas pipelines." *Chemical Engineering Research and Design* (2023).

[25] Rodriguez, O. M. H., and L. S. Baldani. "Prediction of pressure gradient and holdup in wavy stratified liquid–liquid inclined

pipe flow." *Journal of Petroleum Science and Engineering* 96 (2012): 140-151.

[26] Rodriguez, Oscar MH, Iara H. Rodriguez, and Jonas L. Ansoni. "An experimental and numerical study on the wall lubrication force in dispersed liquid-liquid flow." *International Journal of Multiphase Flow* 120 (2019): 103094.

[27] Santos, D. S., P. M. Faia, F. A. P. Garcia, and M. G. Rasteiro. "Oil/water stratified flow in a horizontal pipe: simulated and experimental studies using EIT." *Journal of Petroleum Science and Engineering* 174 (2019): 1179-1193.

[28] Salvi, B. L., and K. A. Subramanian. "A novel approach for experimental study and numerical modeling of combustion characteristics of a hydrogen fuelled spark ignition engine." *Sustainable Energy Technologies and Assessments* 51 (2022): 101972.

[29] Welch, Samuel WJ, and Thami Rachidi. "Numerical computation of film boiling including conjugate heat transfer." *Numerical Heat Transfer: Part B: Fundamentals* 42, no. 1 (2002): 35-53.

[30] Simmons, M. J. H., and B. J. Azzopardi. "Drop size distributions in dispersed liquid–liquid pipe flow." *International journal of multiphase flow* 27, no. 5 (2001): 843-859.

[31] Sharma, M., P. Ravi, Sumana Ghosh, G. Das, and P. K. Das. "Hydrodynamics of lube oil–water flow through 180° return bends." *Chemical engineering science* 66, no. 20 (2011): 4468-4476.

[32] Sharma, M., P. Ravi, Sumana Ghosh, G. Das, and P. K. Das. "Studies on low viscous oil–water flow through return bends." *Experimental thermal and fluid science* 35, no. 3 (2011): 455-469.

[33] Tan, Chao, Feng Dong, Fusheng Zhang, and Wei Li. "Oil-water two-phase flow measurement with a V-cone meter in a horizontal pipe." In 2009 IEEE Instrumentation and Measurement Technology Conference, pp. 62-67. IEEE, 2009.

[34] Tan, Chao, and Feng Dong. "Modification to mass flow rate correlation in oil–water two-phase flow by a V-cone flow meter in consideration of the oil–water viscosity ratio." *Measurement Science and Technology* 21, no. 4 (2010): 045403.

[35] Tan, Jiatong, Jiaqiang Jing, Haili Hu, and Xiangyang You. "Extension of the Roscoe and Brinkman viscosity model for unstable oil-in-water dispersions." *Journal of Dispersion Science and Technology* (2018).

[36] Viggiano, Bianca, Tamara Dib, Nasim Ali, Larry G. Mastin, Raúl Bayoán Cal, and Stephen A. Solovitz. "Turbulence, entrainment and low-order description of a transitional variable-density jet." *Journal of Fluid Mechanics* 836 (2018): 1009-1049.

[37] Voulgaropoulos, Victor, and Panagiota Angeli. "Optical measurements in evolving dispersed pipe flows." *Experiments in Fluids* 58 (2017): 1-15.

[38] Welch, Samuel WJ, and Thami Rachidi. "Numerical computation of film boiling including conjugate heat transfer." *Numerical Heat Transfer: Part B: Fundamentals* 42, no. 1 (2002): 35-53.

[39] Xu, Jing-yu, Dong-hui Li, Jun Guo, and Ying-xiang Wu. "Investigations of phase inversion and frictional pressure gradients in upward and downward oil–water flow in vertical pipes." *International Journal of Multiphase Flow* 36, no. 11-12 (2010): 930-939.

[40] Zhang, Jian, Jing-yu Xu, Ying-xiang Wu, Dong-hui Li, and Hua Li. "Experimental validation of the calculation of phase holdup for an oil–water two-phase vertical flow based on the measurement of pressure drops." *Flow Measurement and Instrumentation* 31 (2013): 96-101.